Superconducting Resonators as Beam Splitters for Linear-Optics Quantum Computation

Luca Chirolli and Guido Burkard
Department of Physics, University of Konstanz, D-78457 Konstanz, Germany

Shwetank Kumar and David P. DiVincenzo
IBM T. J. Watson Research Center, Yorktown Heights, New York 10598, USA
(Received 17 February 2010; published 8 June 2010)

We propose and analyze a technique for producing a beam-splitting quantum gate between two modes of a ring-resonator superconducting cavity. The cavity has two integrated superconducting quantum interference devices (SQUIDs) that are modulated by applying an external magnetic field. The gate is accomplished by applying a radio frequency pulse to one of the SQUIDs at the difference of the two mode frequencies. Departures from perfect beam splitting only arise from corrections to the rotating wave approximation; an exact calculation gives a fidelity of >0.9992. Our construction completes the toolkit for linear-optics quantum computing in circuit quantum electrodynamics.

DOI: 10.1103/PhysRevLett.104.230502 PACS numbers: 03.67.Lx, 84.40.Dc, 85.25.Dq

A functioning quantum computer will be a machine that builds up, in a programmable way, nonclassical correlations in a multipartite quantum system. We now know that there is a remarkable variety of approaches, beyond the straightforward implementation of traditional quantum circuits, for achieving this function. One of these new approaches, linear-optics quantum computation (LOQC) [1,2], has provided an intriguing path forward in traditional quantum optics. In LOQC, all the programmable generation of entanglement is produced by simple, reliable linear optical elements, namely, beam splitters and phase shifters (delay lines). Nonlinear optics is only required in state initialization and detection, in the form of single-photon sources and detectors. These remain difficult to achieve with high fidelity, but are more feasible than the nonlinear Kerr gates that were originally envisioned for optical quantum computation [3].

A new setting for quantum optics has arisen in circuit QED [4]. Research in superconducting (SC) quantum devices, which has led to the discovery of circuit QED, has focused on the nonlinearity provided by the Josephson junction. Josephson qubits have been improving rapidly, and traditional quantum gates of reasonable fidelity have now been reported [5]. But the observation that a Josephson qubit can be strongly coupled to a photon in a SC transmission line resonator [4] opens the way to LOQC implementations using microwave rather than visible photons. Much progress is being made in circuit QED in single-photon sources: Ref. [6] has shown the generation of high-fidelity Fock states in SC transmission line resonators by a high efficiency photon swapping between a qubit and the resonator. Photon detection in circuit QED becomes equivalent to high-fidelity qubit measurement, and this capability has advanced rapidly for SC qubits.

In this Letter we show that the LOQC toolkit in circuit QED can be completed with high-fidelity linear optical elements. We analyze in detail here a realization of a beam splitter; the phase shifter represents a simpler case that can be studied in exactly the same way. We consider photonic modes that are resident in SC resonators. A quantum switch between SC resonators has been proposed in Ref. [7], where a SC qubit mediates an effective second order beam-splitter interaction in the rotating wave approximation (RWA). We look for a way to accomplish such a gate in a high-fidelity controlled way beyond any RWA.

In fact, we show here that high-fidelity beam splitting can be produced in exactly the ring-resonator device analyzed by Ref. [8] [see Fig. 1(a)]. This structure has two nearly degenerate fundamental modes, even and odd with respect to the horizontal midline, with frequencies $\omega_{1,2}$, respectively. The beam-splitting action will take place between photons in these two modes. This ring is interrupted by two SQUIDs as shown. In [8] it is shown that the nonlinearity of these SQUIDs is enough to enable nondemolition measurements, but this nonlinearity is far too small to make a practical traditional quantum gate such as a CPHASE. We can neglect this nonlinearity here, and we will exploit another control available in this device: the effective inductance of these SQUIDs can be controlled by the external magnetic fluxes shown. This inductance couples to the photonic modes by setting the reflection coefficient for standing waves around the ring. It is simply by *modulation* of the inductance of SQUID_1 at the difference frequency $\omega_1 - \omega_2$ that high-fidelity beam-splitting action is achieved [9].

We set up an accurate analysis of the photonic dynamics of our ring resonator by representing the rest of the ring connected to SQUID_1 as a linear, passive structure with two-terminal impedance $Z(\omega)$. Note that we will consider the flux bias of SQUID_2 to be fixed, so that it functions as an inductor with, using the parameters of [8], $L_0 = 0.19$ nH. We neglect losses so that Z is purely imaginary. For device parameters from [8], $Z(\omega)$ can be calculated

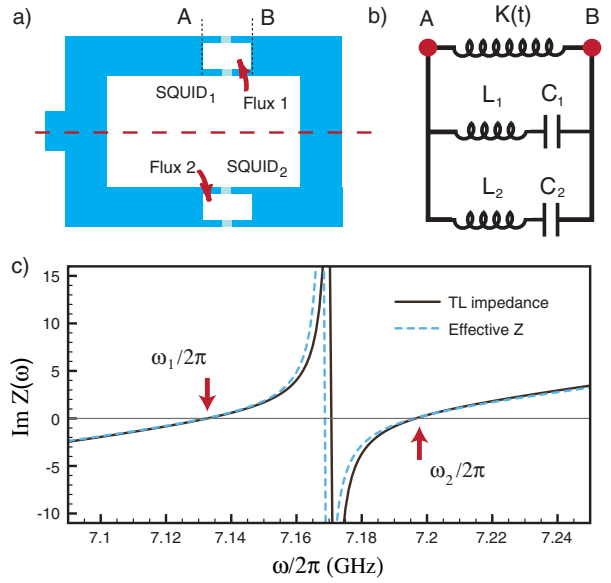

FIG. 1 (color online). (a) Schematic representation of the superconducting ring resonator, comprising two SC transmission line (TL) segments coupled by two SQUIDs that can be externally controlled by two different applied magnetic fluxes. ac modulation of SQUID_1 will accomplish the action of beam splitting between the two fundamental modes of the ring resonator. The device can optionally be tuned by a stub on the midline as shown. (b) Equivalent circuit, consisting of two parametrically coupled LC resonators. The modulation of the SQUID_1 impedance is represented by the time-dependent inductor $K(t)$. The LC circuit parameters are chosen so that the impedance of the two parallel resonators matches the two-terminal impedance, looking down into the AB port, of the ring resonator, in a frequency band including the two fundamental modes. (c) The AB-port impedance of the resonator and of the equivalent circuit. The unmodulated fundamental mode frequencies $\omega_{1,2}$ are given by the two zeros of this impedance.

analytically using standard two-port theory [10]. $\mathrm{Im}Z(\omega)$ in the frequency range of interest is shown in Fig. 1(c). Since we include in Z the inductance L_0 representing the average of the modulated SQUID_1, the two zeros of $Z(\omega)$ correspond to the two mode frequencies $\omega_{1,2}$ of the unmodulated ring resonator.

This impedance is extremely well reproduced (dashed line) by that of the two-pole structure in our equivalent circuit shown in Fig. 1(b). This fit is obtained with parameters $L_1 = 5.8$ nH, $C_1 = 86$ fF, $L_2 = 7.7$ nH, and $C_2 = 63$ fF. It is practical for the amplitude of the parametrically modulated inductance $K(t)$ to be around 0.04 nH. We can apply our network graph theory [11] to analyze the quantum behavior of these modes of the ring resonator. The classical time-dependent Hamiltonian that describes the equivalent circuit Fig. 1(b) is

$$H = \sum_{i=1,2}\left(\frac{Q_i^2}{2C_i} + \frac{\Phi_i^2}{2L_i}\right) - \frac{K(t)}{2}\left(\frac{\Phi_1}{L_1} + \frac{\Phi_2}{L_2}\right)^2. \quad (1)$$

We choose the time-dependent inductance to have the form $K(t) = \delta K \cos(\omega_d t)$. We will present calculations only for the case where δK is switched on from zero at $t = 0$, then switched off again at $t = \tau$. We will see that even for such an unshaped, square modulation pulse, the desired quantum gate operation can be achieved with excellent fidelity. We find that this fidelity is insensitive to details of pulse shaping.

We quantize Eq. (1) by imposing commutation rules between canonically conjugate variables $[\hat{\Phi}_i, \hat{Q}_j] = i\hbar\delta_{ij}$ and express them, using creation and annihilation operators $a^\dagger$ and a, as $\hat{\Phi}_i = \sigma_i\sqrt{\hbar}(a_i + a_i^\dagger)/\sqrt{2}$, and $\hat{Q}_i = -i\sqrt{\hbar}(a_i - a_i^\dagger)/\sqrt{2}\sigma_i$, with $\sigma_i = (L_i/C_i)^{1/4}$. Assuming $K(t) \ll L_{1,2}$, the Hamiltonian becomes ($\hbar = 1$)

$$H = \sum_{i=1,2}\omega_i a_i^\dagger a_i + f(t)[\lambda(a_1 + a_1^\dagger) + \frac{1}{\lambda}(a_2 + a_2^\dagger)]^2. \quad (2)$$

Here the two resonant harmonic frequencies are $\omega_i = 1/\sqrt{L_i C_i}$, $\lambda = (L_2^3 C_2/L_1^3 C_1)^{1/8}$, and $f(t) = -\sigma_1\sigma_2 K(t)/4L_1L_2 \equiv f\cos(\omega_d t)$. We will consider driving at resonance at transition frequency $\omega_d = \Delta\omega = \omega_1 - \omega_2$. For the ring resonator we will always be in the regime $\Delta\omega \ll \omega_1, \omega_2$.

To study the beam-splitting action created by the $K(t)$ pulse, we will calculate the time evolution of an initial state comprising a single photon in one of the two modes (mode 1), i.e., $|\psi_i\rangle = a_1^\dagger|0\rangle$, with $|0\rangle = |0\rangle_1|0\rangle_2$. We aim for the final "beam-split" state $|\psi_f\rangle = \frac{1}{\sqrt{2}}(a_1^\dagger - ia_2^\dagger)|0\rangle$. We consider always a doubly rotating frame with rotation at frequency $\omega_{1,2}$ for modes 1, 2, respectively. We will study a fidelity $\mathcal{F}(\tau) = |\langle\psi_f|\mathcal{U}(\tau)|\psi_i\rangle|^2$, which indicates how close to ideal beam splitting our operation is. Here, $\mathcal{U}(t) = \mathcal{T}\exp[-i\int^t dt' H(t')]$ denotes the evolution operator generated by the Hamiltonian Eq. (2). The use of more general gate fidelities would not affect our conclusions.

We present three approaches to the calculation of $\mathcal{F}(\tau)$. First we perform a naive RWA in which only time-independent terms in the rotating frame are retained in $H(t)$. An elementary calculation gives $\mathcal{F}_{\mathrm{RWA}}(\tau) = [1 + \sin(2f\tau)]/2$. Given the smallness of $\Delta\omega$, a second calculation is much more accurate, which retains additional terms in the rotating frame that oscillate at frequencies $\Delta\omega$ and $2\Delta\omega$. Then the part of the Hamiltonian that generates the beam-splitting gate is

$$H_{\mathrm{BS}} = f a_1 a_2^\dagger(1 + e^{-2i\Delta\omega t}) + \mathrm{H.c.} \quad (3)$$

The terms oscillating at frequency $2\Delta\omega$ produce Bloch-Siegert oscillations (BSO) [12]. For $f \ll \Delta\omega$ these can be treated perturbatively [13]. By considering virtual transitions via the first two sidebands shifted in energy by $\pm 2\Delta\omega$, the fidelity at first order in $f/\Delta\omega$ is

$$\mathcal{F}_{\mathrm{BSO}}(\tau) = \frac{1}{2}\left[1 + \sin(2f\tau) + \frac{f}{\Delta\omega}\cos(2f\tau)\sin(2\Delta\omega\tau)\right]. \quad (4)$$

Within both the RWA and the BSO approximations, for a pulse of duration $\tau = \pi/4f$ we attain $\mathcal{F} = 1$: beam splitting is perfect at these levels of approximation. There is a real difference between these two points of view; in the naive RWA the Bloch vector in the $|01\rangle - |10\rangle$ space undergoes simple circular motion, while the BSO manifest themselves as a nutational motion of the Bloch vector (Fig. 2). But in both cases the Bloch vector arrives exactly at the equator. Note that in both cases the Rabi oscillation frequency $\Omega_R = 2f$ has the simple form

$$\Omega_R = \frac{\delta K}{2}\sqrt{\frac{\omega_1\omega_2}{L_1L_2}}. \tag{5}$$

For the parameters of our ring resonator, this gives a very convenient value of $\Omega_R/2\pi \approx 20$ MHz.

Unfortunately, the actual time evolution of our Hamiltonian does not give 100% fidelity for beam splitting. Parametric time-dependent modulation causes mode squeezing; in other words, photon number is not conserved, and our evolution does not remain confined to the $|01\rangle - |10\rangle$ Bloch sphere. To quantify this effect, we must do a third calculation that goes beyond any rotating wave approximation. With only a modest amount of numerical effort, it is feasible to do an essentially exact calculation of our gate operation. All that is required is a 4×4 matrix calculation of the Heisenberg operators $a_{1,2}(t)$ and $a^\dagger_{1,2}(t)$ [14]. This calculation begins by using the canonically conjugate quadratures $\boldsymbol{\xi} = (\hat{q}_1, \hat{q}_2, \hat{p}_1, \hat{p}_2)^T$ that are related to the original fluxes and charges by $(\hat{\Phi}_1, \hat{\Phi}_2, \hat{Q}_1, \hat{Q}_2)^T = \sqrt{\hbar} D_\sigma \boldsymbol{\xi}$, with the diagonal matrix $D_\sigma = \mathrm{diag}(\sigma_1, \sigma_2, 1/\sigma_1, 1/\sigma_2)$. Because the Hamiltonian governing the evolution is quadratic, the Heisenberg equations of motion for the quadratures $\boldsymbol{\xi}$ are linear,

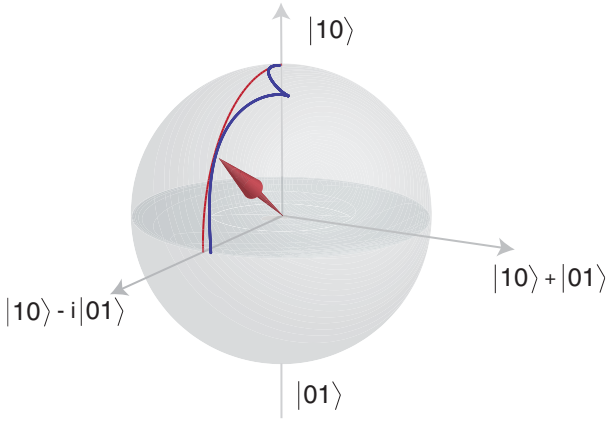

FIG. 2 (color online). To good approximation, the quantum evolution is confined to the Bloch sphere defined by the $|01\rangle$ and $|10\rangle$ states. Counterrotating terms in the Hamiltonian at frequency $2\Delta\omega$ perturb the simple Bloch-sphere (red) evolution by terms of order $f/\Delta\omega$. Bloch-Siegert oscillations (blue; with cusp) cause nutation of the Bloch vector superimposed on regular precession in the rotating frame. The device parameters for the ring resonator are as given in the text.

$$\dot{\boldsymbol{\xi}} = \Xi(t)\boldsymbol{\xi} = \begin{pmatrix} 0 & \Omega \\ -\Omega - 4f(t)\Lambda & 0 \end{pmatrix}\boldsymbol{\xi}, \tag{6}$$

where Λ and Ω are real 2×2 matrices with $\Omega = \mathrm{diag}(\omega_1, \omega_2)$, $\Lambda_{11} = \lambda^2$, $\Lambda_{22} = 1/\lambda^2$, and $\Lambda_{12} = \Lambda_{21} = 1$. The general solution can be expressed in terms of $S(t) = \mathcal{T}\exp\int^t dt' \Xi(t')$, where $S(t)$ is a 4×4 real symplectic matrix that satisfies $S^T(t) J S(t) = J$, with the 4×4 real antisymmetric matrix J having a 2×2 block structure, with $J_{12} = -J_{21} = \mathbb{1}$ and $J_{11} = J_{22} = 0$.

The action of the evolution operator $\mathcal{U}(t)$ on the canonical quadratures $\boldsymbol{\xi}$ results in a matrix multiplication $\boldsymbol{\xi}(t) = \mathcal{U}^\dagger(t)\boldsymbol{\xi}\mathcal{U}(t) = S(t)\boldsymbol{\xi}$ that connects the Heisenberg and the Schrödinger representation. A similar relation holds for the field operators a_i and $a_i^\dagger$. By defining the vector $\mathbf{a} = (a_1, a_2, a_1^\dagger, a_2^\dagger)^T$, the connection between the Heisenberg and the Schrödinger representation reads as $\mathbf{a}(t) = S_{(c)}(t)\mathbf{a}$, with $S_{(c)}(t) = \Sigma^\dagger S(t)\Sigma$, where Σ is the simple unitary matrix of the basis change $\boldsymbol{\xi} = \Sigma\mathbf{a}$.

Here we show that the real symplectic matrix $S(t)$ contains all the information needed to calculate the fidelity $\mathcal{F}(\tau) = |\langle\psi_f|\mathcal{U}(t)|\psi_i\rangle|^2$ exactly. Any real symplectic matrix $S \in \mathrm{Sp}(4, \mathbb{R})$ admits a singular value decomposition in terms of real orthogonal symplectic matrices, $S = S_L D S_R^T$, with $S_\alpha^T S_\alpha = \mathbb{1}$, $S_\alpha^T J S_\alpha = J$, for $\alpha = L, R$, and $D = \mathrm{diag}(\kappa_1, \kappa_2, 1/\kappa_1, 1/\kappa_2)$, which is unique up to a reordering of the diagonal entries of D [15]. This decomposition of S induces a corresponding decomposition of the evolution operator $\mathcal{U}(S)$: $\mathcal{U}(S) = \mathcal{U}(S_L)\mathcal{U}(D)\mathcal{U}^\dagger(S_R)$. The elements S_α $(\alpha = L, R)$ have the general 2×2 block form $[S_\alpha]_{11} = [S_\alpha]_{22} = X_\alpha$ and $[S_\alpha]_{12} = -[S_\alpha]_{21} = Y_\alpha$, with X_α, Y_α real 2×2 matrices such that $U_\alpha \equiv X_\alpha - iY_\alpha$ is a unitary 2×2 matrix [16,17].

It follows that the unitary evolution $\mathcal{U}(S_\alpha)$ associated with S_α conserves the number of photons and does not mix the creation and annihilation operators: $\mathcal{U}^\dagger(S_\alpha) a_i \mathcal{U}(S_\alpha) = \sum_{k=1,2}[U_\alpha]_{jk} a_k$ [18]. On the other hand, the diagonal matrix D represents an active term that introduces squeezing in the two modes. In terms of mode operators $\mathcal{U}(D)$ can be expressed using independent squeezing operators $\Pi_i(\rho) = \exp[\rho(a_i^2 - a_i^{\dagger 2})/2]$: $\mathcal{U}(D) = \mathcal{U}(\kappa_1, \kappa_2) = \Pi_1(-\ln\kappa_1)\Pi_2(-\ln\kappa_2)$. Its action on the mode annihilation operators is simply given by $\Pi_i^\dagger(\rho) a_i \Pi_i(\rho) = a_i \cosh\rho - a_i^\dagger \sinh\rho$. These facts allow us to write the fidelity as

$$\mathcal{F} = |\langle\Psi_f|\mathcal{U}(\kappa_1, \kappa_2)|0\rangle|^2, \tag{7}$$

with the state $|\Psi_f\rangle = (b_1^+ + b_2^+)|00\rangle/\sqrt{2} + (b_1^- + b_2^-)|11\rangle/\sqrt{2} - b_1^-|20\rangle - b_2^-|02\rangle$ with $b_j^\pm = \delta_j(\kappa_j^2 \pm 1)/2\kappa_j$ and $\delta_j = [U_R]_{1j}([U_L]_{1j} + i[U_L]_{2j})^*$ for $j = 1, 2$. Equation (7) can now be evaluated in closed form, because the two-mode squeezed vacuum $\mathcal{U}(\kappa_1, \kappa_2)|0\rangle$ has an analytical expression in the Fock space via the relation [14]

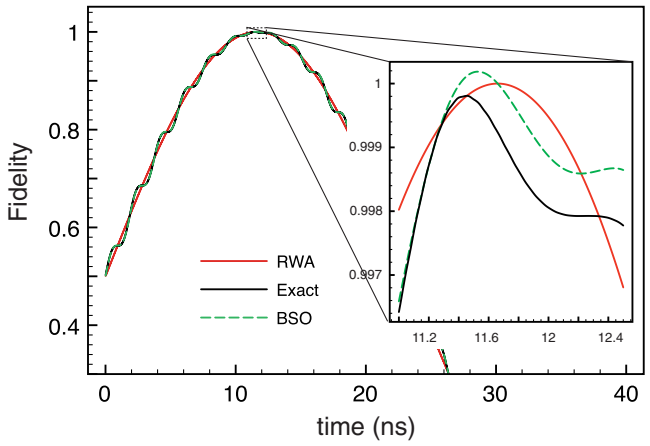

FIG. 3 (color online). Fidelity of the beam-splitting gate as a function of pulse duration, using a naive rotating wave approximation (RWA), a rotating wave approximation including some additional slow-rotating terms perturbatively, capturing the occurrence of Bloch-Siegert oscillations (BSO), in comparison with the numerically exact solution. Note that since the BSO result reproduces the exact result with large precision, the two lines lie essentially on top of each other in the main panel and can only be distinguished in the magnified plot (inset). Because of its simple perturbative nature, the BSO fidelity can (and does) exceed 1. The fidelity can be further optimized by carefully adjusting the resonator frequencies and thus the phase of the BSO. The device parameters for the ring resonator are as given in the text, except that stub tuning is used to raise the mode splitting to $\Delta\omega \approx 260$ MHz.

$$\langle n|\Pi(\rho)|0\rangle = \frac{(\tanh\rho)^{n/2}}{2^{n/2}(n!\cosh\rho)^{1/2}} H_n(0), \tag{8}$$

with $H_n(0)$ the Hermite polynomial at the origin, which is zero for odd n and $H_n(0) = (-1)^{n/2} n!/(n/2)!$ for even n. Therefore, after a singular value deomposition of S the fidelity is directly obtained as a simple function of the quantities κ_i and δ_i.

Figure 3 shows our three calculations of the beam-splitting fidelity as a function of pulse duration time τ. The device parameters for the ring resonator are as given above, except that by introducing an electrical stub for tuning as in Fig. 1(a) the frequency of the even-symmetry mode $\omega_1/2\pi$ is lowered to around 6.93 GHz, so that $\Delta\omega/2\pi \approx 260$ MHz. We see that the evolution approximately follows the smooth Rabi oscillation predicted by the naive RWA, but that there are appreciable BSO superimposed on this. The perturbative BSO calculation in fact comes very close to the exact evolution for our parameters. The exact calculation gives an extremely high value of the fidelity: $\mathcal{F}_{\max} > 0.9992$. Squeezing is very small because the parametric modulation frequency is very slow compared with the mode frequencies ($\Delta\omega \ll \omega_{1,2}$). For the ring resonator without the stub this ratio is even smaller, since then $\Delta\omega \approx 64$ MHz, but this device is awkward to use since then the BSO become very large and are no longer well described perturbatively [19].

To summarize, we see that for a very straightforward ring-resonator geometry, almost ideal beam splitting between two cavity modes can be readily achieved. The calculated fidelity of 0.9992 is not realistic; other limits such as resonator loss and $1/f$ noise would come into play at this level for the present state of the art. But our result shows that there is no intrinsic limit to accomplishing effective beam splitting by device modulation. Finally, we mention that an effective "delay line" is also readily implemented in this device; by transiently changing the dc bias fluxes of the two SQUIDs, in either an even or an odd fashion, either mode may be subjected to any desired phase shift. There will be even less intrinsic limitation on the fidelity of these operations. Thus, we see that the toolkit for LOQC is readily completable in SC microwave circuits.

Financial support from SFB 767 "Controlled Nanostructures" and the Konstanz Center for Applied Photonics (CAP) are gratefully acknowledged. This research was supported in part by the National Science Foundation under Grant No. PHY05-51164.

[1] E. Knill, R. Laflamme, and G. J. Milburn, Nature (London) **409**, 46 (2001).
[2] P. Kok *et al.*, Rev. Mod. Phys. **79**, 135 (2007).
[3] G. J. Milburn, Phys. Rev. Lett. **62**, 2124 (1989).
[4] A. Wallraff *et al.*, Nature (London) **431**, 162 (2004).
[5] L. DiCarlo *et al.*, Nature (London) **460**, 240 (2009).
[6] M. Hofheinz *et al.*, Nature (London) **459**, 546 (2009).
[7] M. Mariantoni *et al.*, Phys. Rev. B **78**, 104508 (2008).
[8] S. Kumar and D. P. DiVincenzo, arXiv:0906.2979.
[9] For another scheme for achieving such modulation, see N. Bergeal *et al.*, arXiv:0805.3452; arXiv:0912.3407.
[10] R. E. Collins, *Foundations for Microwave Engineering* (Wiley, New York, 2001), Sec. 4.9.
[11] G. Burkard, R. H. Koch, and D. DiVincenzo, Phys. Rev. B **69**, 064503 (2004).
[12] F. Bloch and A. Siegert, Phys. Rev. **57**, 522 (1940).
[13] M. S. Shahriar, P. Pradhan, and J. Morzinski, Phys. Rev. A **69**, 032308 (2004).
[14] M. O. Scully and M. S. Zubairy, *Quantum Optics* (Cambridge University Press, Cambridge, England, 1997).
[15] H. Xu, Linear Algebra Appl. **368**, 1 (2003).
[16] The elements S_α belong to the maximally compact subgroup K(2) of Sp(4, $\mathbb{R}$) that is isomorphous to U(2), K(2) = SO(4) $\cap$ Sp(4, $\mathbb{R}$) = U(2).
[17] R. Simon, N. Mukunda, and B. Dutta, Phys. Rev. A **49**, 1567 (1994).
[18] Arvind, B. Dutta, N. Mukunda, and R. Simon, Phys. Rev. A **52**, 1609 (1995).
[19] G. D. Fuchs, V. V. Dobrovitski, D. M. Toyli, F. J. Heremans, and D. D. Awschalom, Science **326**, 1520 (2009).